Supplementary Information (SI) for Polymer Chemistry.

Long-Stable Lithium Metal Batteries with a High-Performance Dual-Salt Solid Polymer Electrolyte

Supporting Information

S1. Calculation of ionic conductivity

The Li-ion conductivities of the electrolytes were acquired by EIS measurements (from 10^5 Hz to 10^{-2} Hz) at a temperature range of 20-80 ºC. The ionic conductivities of the membranes were calculated according to the following equation (S1):

$$\sigma = \frac{d}{R_b A} \qquad (S1)$$

where d is the film thickness, R_b is the electrolyte impedance, and A is the electrode area.

S2. Calculation of activation energy

The activation energy is used to demonstrate the difficulty of lithium-ion transfer. It is derived using the Arrhenius equation (S2):

$$\sigma = \sigma_0 \exp\left(-\frac{E_a}{RT}\right) \qquad (S2)$$

where Ea is the activation energy, T is the test temperature, and R is the Boltzmann constant.

S3. Calculation of Li^+ transference numbers

The Li^+ transfer numbers (t_{Li+}) of the electrolytes were tested using Li|SPE|Li symmetric cells. t_{Li+} values are calculated from equation (S3):

$$t_{Li}^{+} = \frac{I_{ss}(\Delta V - I_0 R_0)}{I_0(\Delta V - I_{ss} R_{ss})} \qquad (S3)$$

where ΔV is the applied polarization voltage (10 mV), I_0 and R_0 are the initial current and initial interface resistance respectively, and I_{SS} and R_{SS} are the post-polarization steady-state current and interface resistance respectively.

Fig. S1. Optical images of PVDF-HFP nanofiber membrane and the measurement of the thickness.

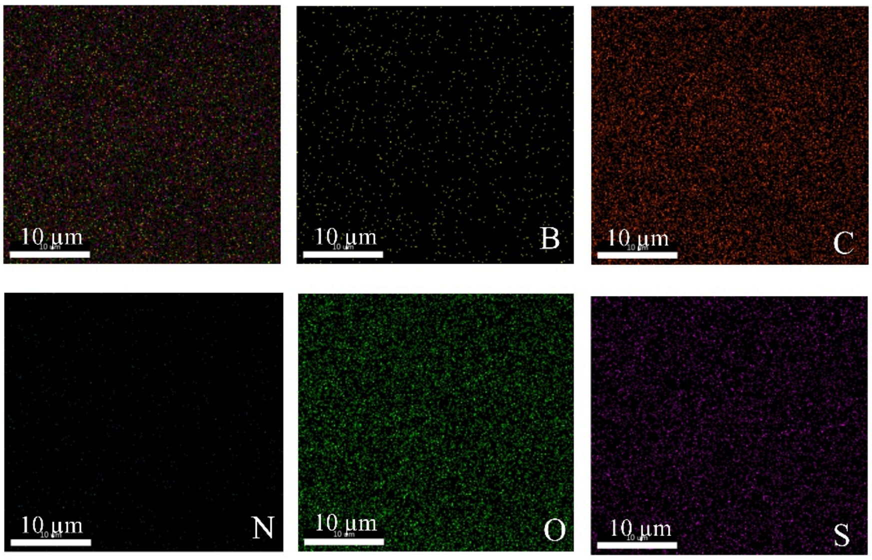

Fig. S2. EDS mappings of $N_2V_8L_{1\text{-}0.1}$ SPE.

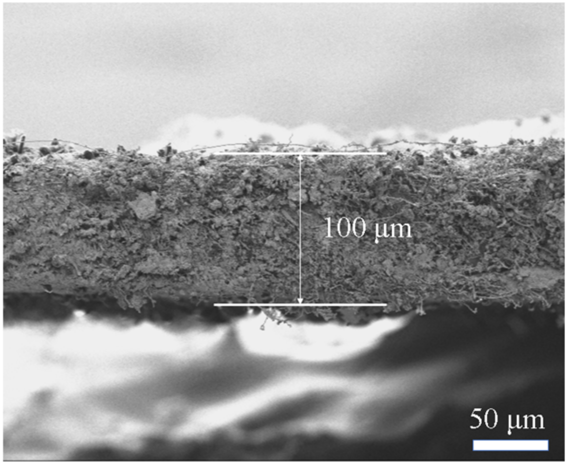

Fig. S3. Cross-sectional SEM image of the $N_2V_8L_{1\text{-}0.1}$ SPE membrane.

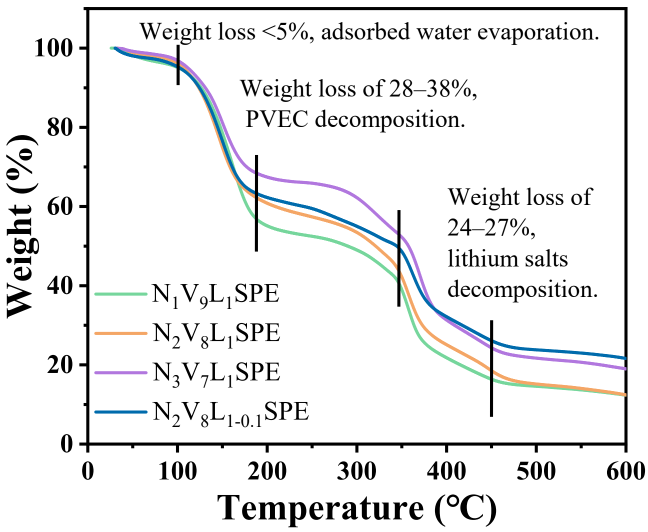

Fig. S4. TG curves of $N_1V_9L_1$, $N_2V_8L_1$, $N_3V_7L_1$ and $N_2V_8L_{1\text{-}0.1}$ SPEs.

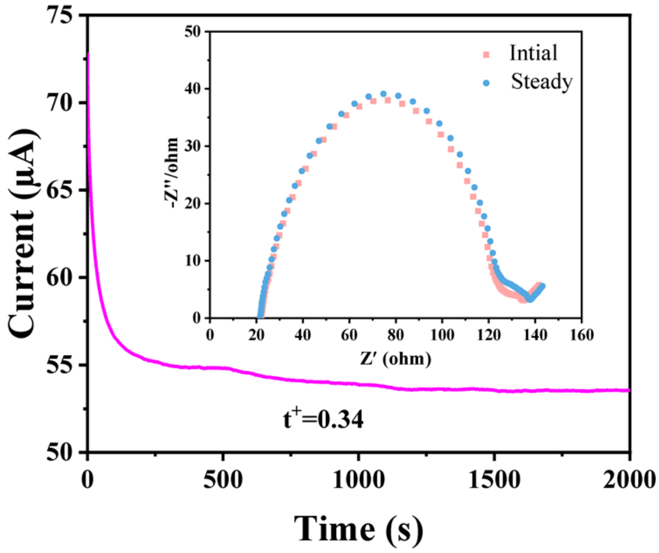

Fig. S5. The current-time curve for a Li|$N_2V_8L_1$ SPE|Li symmetrical cell with an applied polarization voltage of 10 mV and the corresponding EIS spectra before and after polarization.

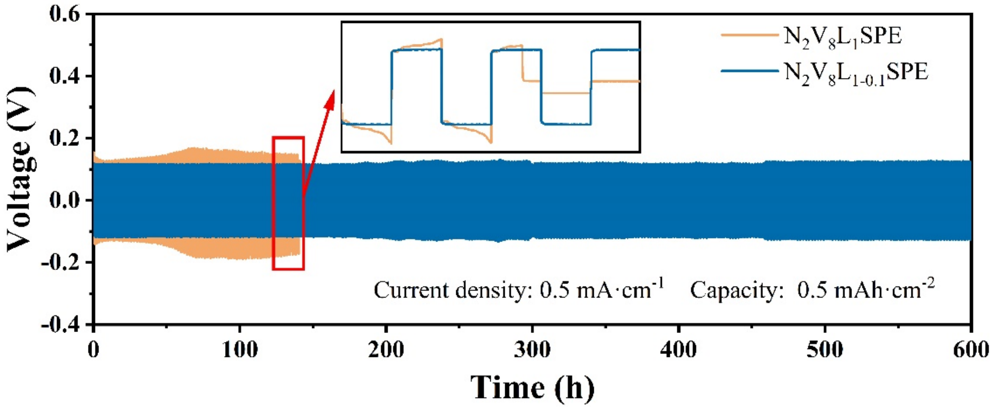

Fig. S6. Long-term constant current cycling plots of Li|$N_2V_8L_1$ SPE|Li and Li|$N_2V_8L_{1-0.1}$ SPE|Li cells at 0.5 mA cm^{-2}.

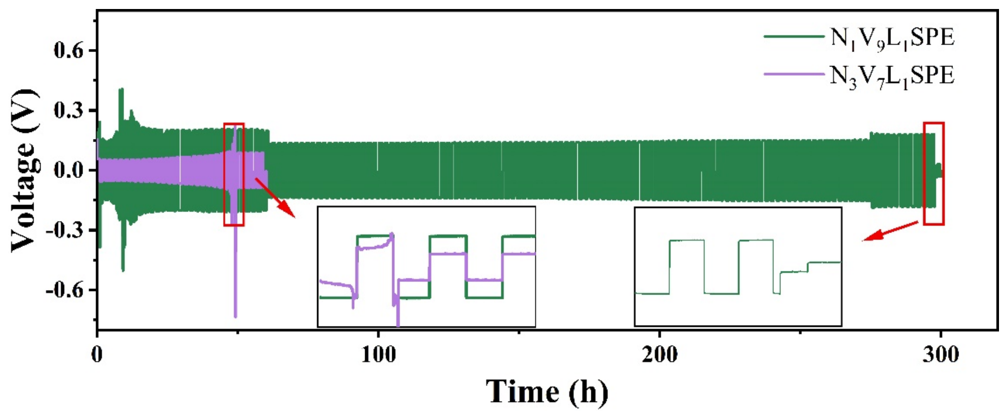

Fig. S7. Long-term constant current cycling of Li|SPE|Li cells with single-salt $N_1V_9L_1$ and $N_3V_7L_1$ SPEs at 0.1 mA cm^{-2}.

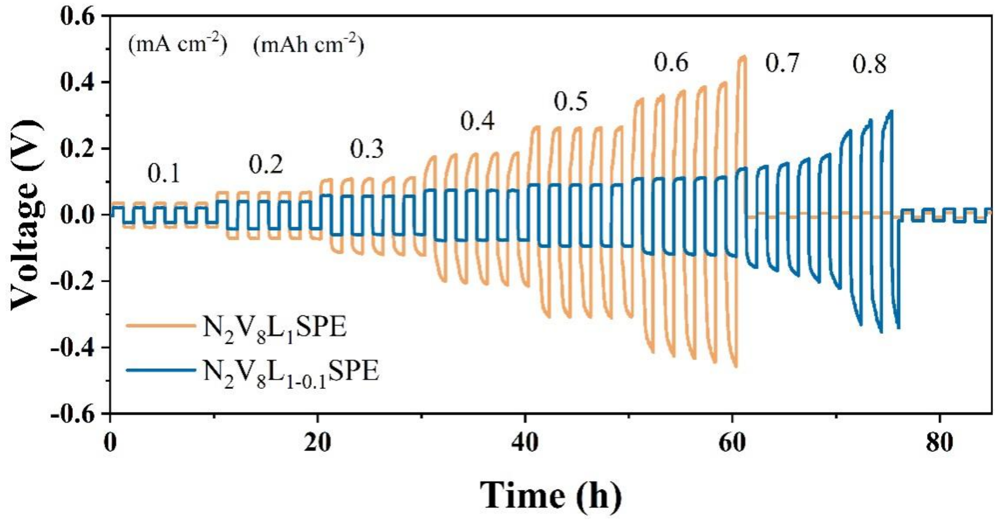

Fig. S8. CCD measurements of Li|$N_2V_8L_1$ SPE|Li and Li|$N_2V_8L_{1-0.1}$ SPE|Li cells.

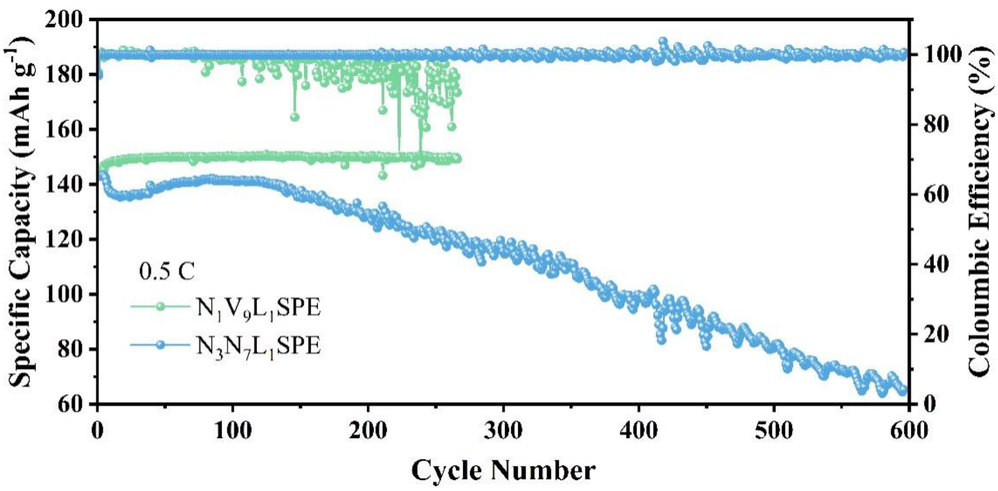

Fig. S9. Long-term cycling plots of Li|$N_1V_9L_1$ SPE|LFP and Li|$N_3V_7L_1$ SPE|LFP cells at 0.5 C.

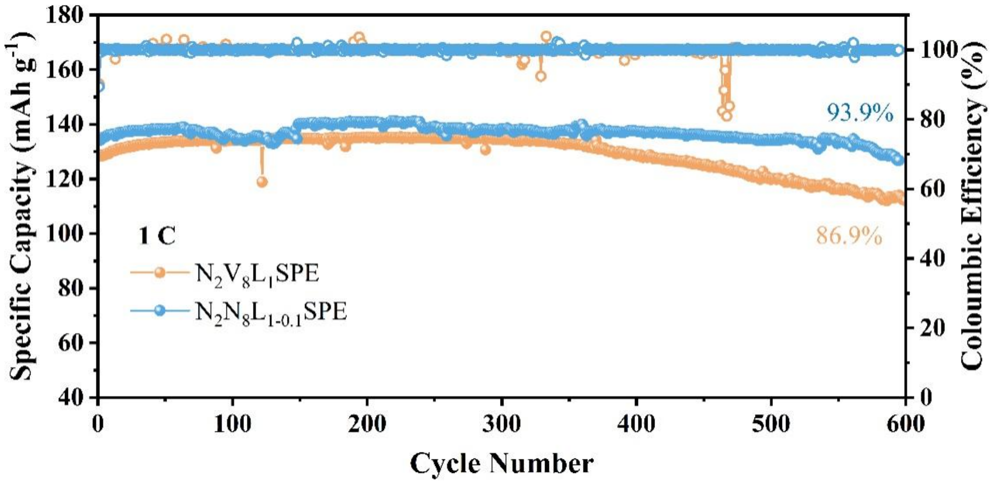

Fig. S10. Long-term cycling plots of Li|$N_2V_8L_1$ SPE|LFP and Li|$N_2V_8L_{1\text{-}0.1}$ SPE|LFP battery at 1 C.

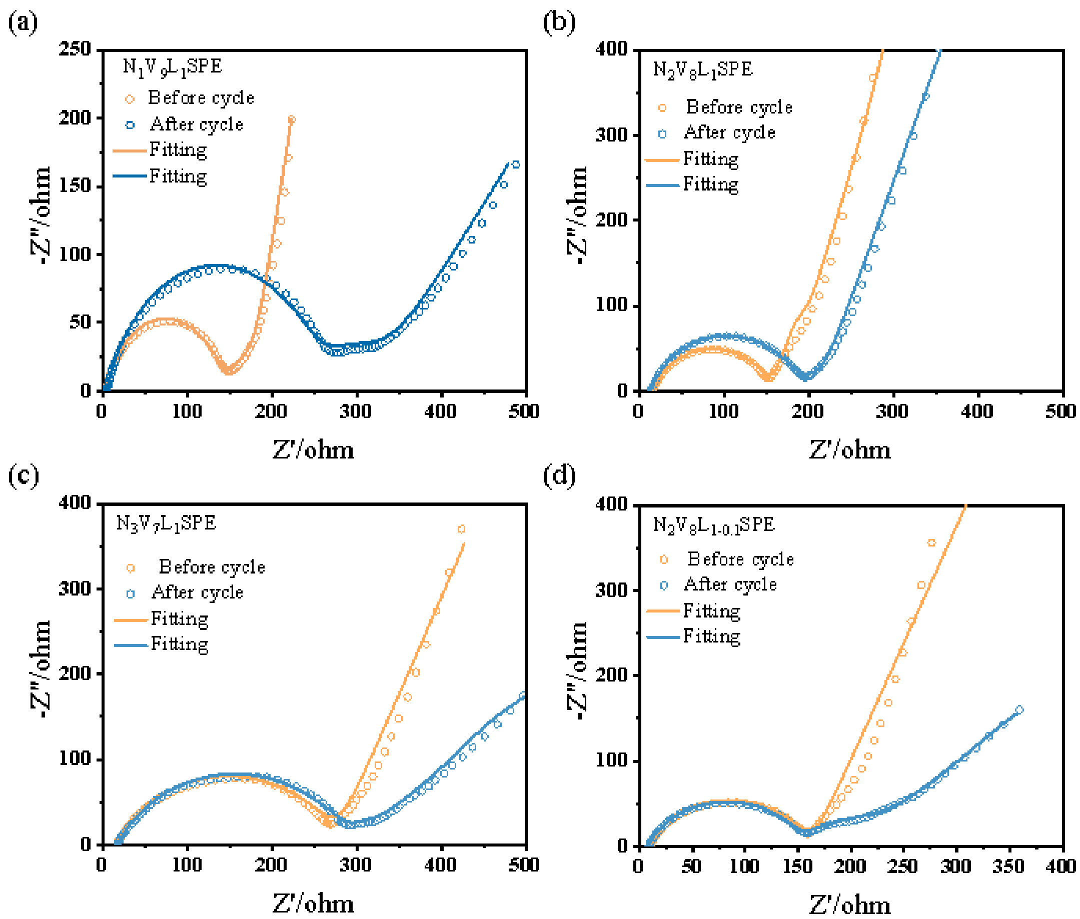

Fig. S11. EIS plots and the fitting curves of (a) Li|$N_1V_9L_1$ SPE|LFP, (b) Li|$N_2V_8L_1$ SPE|LFP, (c) Li|$N_3V_7L_1$ SPE|LFP, (d) Li|$N_2V_8L_{1\text{-}0.1}$ SPE|LFP before and after cycling.

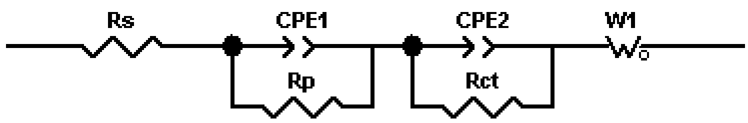

Fig. S12. Equivalent circuit model for EIS fitting.

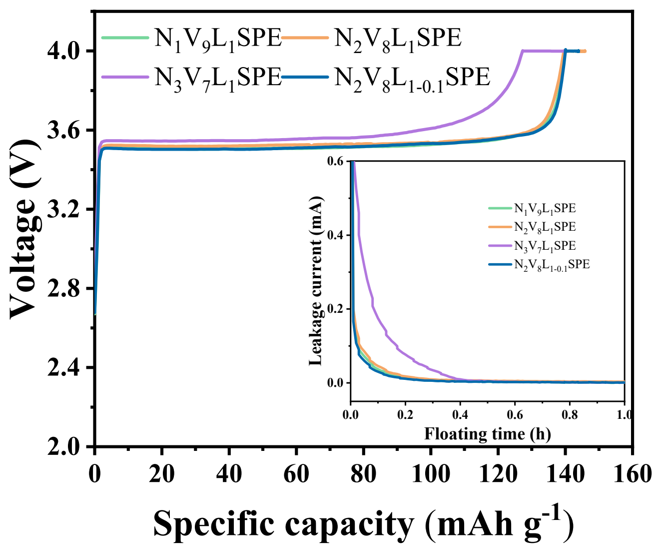

Fig.S13. The charge curves and leakage current plots (inset) of Li||LFP batteries with different SPEs at a constant voltage of 4.0 V.

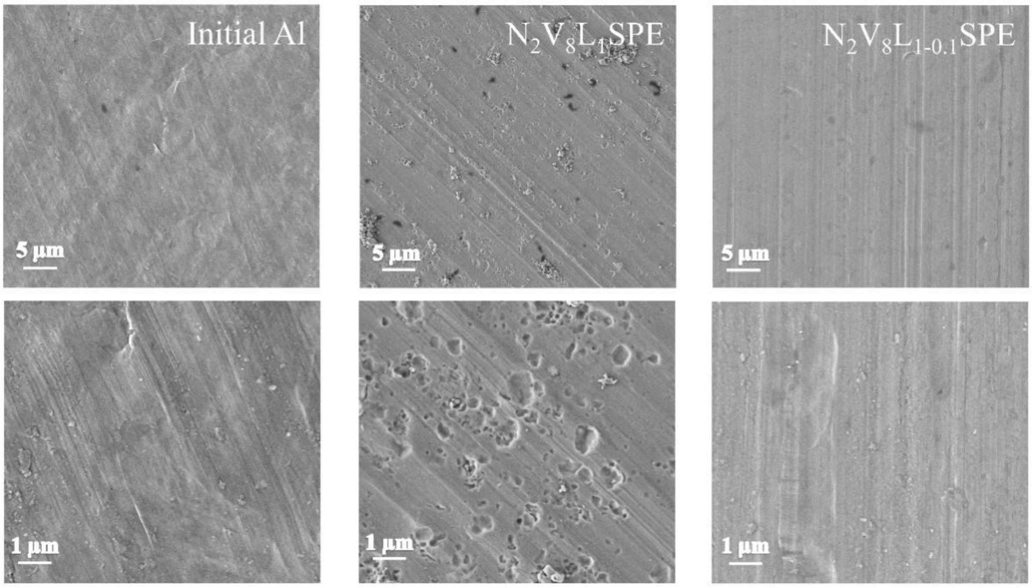

Fig. S14. SEM images of (a) the initial Al collector and the cycled Al collectors with (b) $N_2V_8L_1$ SPE and (c) $N_2V_8L_{1-0.1}$ SPE after 300 cycles.

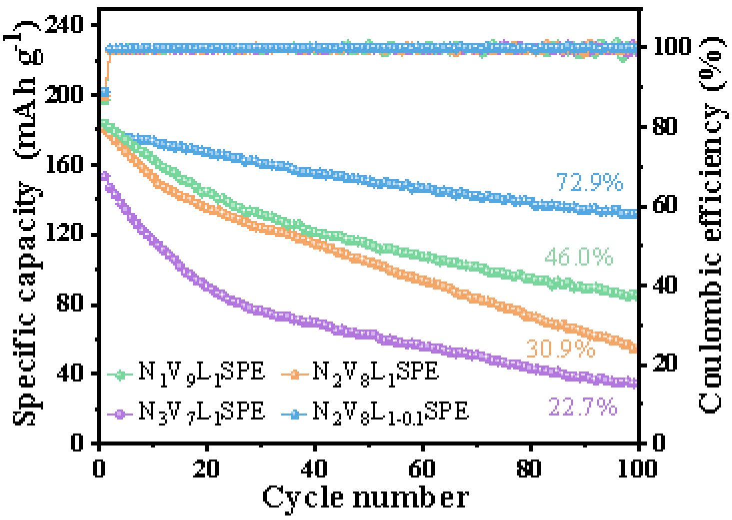

Fig. S15. Cycling stability of Li||NCM811 cells with $N_1V_9L_1$, $N_2V_8L_1$, $N_3V_7L_1$ and $N_2V_8L_{1-0.1}$ SPEs at 0.5 C.

Table S1. Comparison of crosslinking degrees of SPEs.

SPEs	T2A (ms)	T2B (ms)	Crosslinking percentage (%)	Pendulum chain percentage (%)	Crosslinking density (*E-4mol/ml)
$N_1V_9L_1$	18.12	847.53	4.44	95.56	0.043
$N_2V_8L_1$	62.12	415.11	9.19	90.81	0.044
$N_3V_7L_1$	11.49	52.22	13	87	0.351
$N_2V_8L_{1\text{-}0.1}$	27.51	108.56	17.47	82.53	0.17

Table. S2. The mechanical property data for $N_2V_8L_{1\text{-}0.1}$ SPE, $N_2V_8L_1$ SPE and PVDF-HFP memabrane.

SPEs	Young's modulus (MPa)	Elongation at break (%)	Tensile Strength (MPa)	Tensile Fracture Stress (MPa)
$N_2V_8L_{1\text{-}0.1}$ SPE	10.77	120.71	12.18	7.32
$N_2V_8L_1$ SPE	9.31	124.22	11.1	7.91
PVDF-HFP	6.23	211.2	9.71	5.85

Table S3. Impedance data of different Li||LFP cells.

Style	Before cycle		After cycle	
	R_{bulk} (Ω)	$R_{interphase}$ (Ω)	R_{bulk} (Ω)	$R_{interphase}$ (Ω)
Li|$N_1V_9L_1$ SPE|LFP	4.8	147.48	4.8	276.8
Li|$N_2V_8L_1$ SPE|LFP	16.1	153.4	14.2	197.4
Li|$N_3V_7L_1$ SPE|LFP	18.0	272.1	19.11	295.7
Li|$N_2V_8L_{1\text{-}0.1}$ SPE|LFP	10.5	160.1	9.1	157.2

Table. S4. Electrochemical performance of different SPEs reported in literature.

SPE ingredients	Voltage window (V)	Room temperature ionic conductivity (10^{-4} S·cm^{-1})	Cell(cycles)capacity retention/C-rate
$Ni_3B_2O_3$/PEO[1]	6.00	0.85	Li||LFP (80 th) 97.5%/0.2 C
LiFSI-DOL[2]	4.70	7.90	Li||LFP (500 th) 69.3%/1 C
Pyr_{14}TFSI/PEO[3]	4.50	3.98	Li||LFP (100 th) 82.9%/0.5 C
PEO-LiPCSI[4]	5.53	/	Li||LFP (85 th) 80%/0.1 C
Poly (diethylene	/	1.6	LFP||Li (100 th)

glycol carbonate)[5]			95%/0.2 C
PCL-LiTFSI[6]	4.6	0.25	NCM622‖Li (100 th) 81.6%/0.1 C
LiTFPFB/P(PO/EM)[7]	4.6	1.55	Li‖LFMP (100th) 88.7%/0.1 C
PEO/LDH[8]	5	1.1	Li‖LFP (100 th) 88%/0.2 C
PEO-LATP[9]	5	0.12	Li‖LFP (50 th) 84%/0.1 C
UV-PCCE[10]	4.78	9.1	Li‖LFP (180 th) 83.9%/0.5 C
PEO-cPTFBC[11]	4.7	2.2	Li‖LFP (150 th) 98.2%/0.1 C
NPGDA-VEC/PVDF-HFP (This work)	5.10	2.64	Li‖LFP (1400 th) 98.4%/0.5 C

References

1 Z. Guo, Y. Wu, X. Li, X. Wu, Q. Hu, Z. Wang, H. Guo, W. Peng, G. Yan and J. Wang, *Ionics*, 2022, **28**, 779–788.

2 H. Cheng, J. Zhu, H. Jin, C. Gao, H. Liu, N. Cai, Y. Liu, P. Zhang and M. Wang, *Mater. Today Energy*, 2021, **20**, 100623.

3 L. Tian, M. Wang, Y. Liu, Z. Su, B. Niu, Y. Zhang, P. Dong and D. Long, *J. Power Sources*, 2022, **543**, 231848.

4 H. Yuan, J. Luan, Z. Yang, J. Zhang, Y. Wu, Z. Lu and H. Liu, *ACS Appl. Mater. Interfaces*, 2020, **12**, 7249–7256.

5 X. Liu, G. Ding, X. Zhou, S. Li, W. He, J. Chai, C. Pang, Z. Liu and G. Cui, *J. Mater. Chem. A*, 2017, **5**, 11124–11130.

6 Y. Seo, Y.-C. Jung, M.-S. Park and D.-W. Kim, *J. Membr. Sci.*, 2020, **603**, 117995.

7 Q. Wang, Z. Cui, Q. Zhou, X. Shangguan, X. Du, S. Dong, L. Qiao, S. Huang, X. Liu, K. Tang, X. Zhou and G. Cui, *Energy Storage Mater.*, 2020, **25**, 756–763.

8 Q. Wang, J.-F. Wu, Z.-Y. Yu and X. Guo, *Solid State Ion.*, 2020, **347**, 115275.

9 L. Liu, L. Chu, B. Jiang and M. Li, *Solid State Ion.*, 2019, **331**, 89–95.

10 Y. Lu, K.-W. He, S.-J. Zhang, Y.-X. Zhou and Z.-B. Wang, *Ionics*, 2019, **25**, 1607–1615.

11 Q. Wang, X. Liu, Z. Cui, X. Shangguan, H. Zhang, J. Zhang, K. Tang, L. Li, X. Zhou and G. Cui, *Electrochimica Acta*, 2020, **337**, 135843.